



Theoretical study on the proton shuttle mechanism of saccharopine dehydrogenase



Xiang Sheng^a, Jun Gao^a, Yongjun Liu^{a,b,*}, Chengbu Liu^a

^a Key Laboratory of Theoretical and Computational Chemistry in Universities of Shandong, School of Chemistry and Chemical Engineering, Shandong University, Jinan, Shandong 250100, China

^b Northwest Institute of Plateau Biology, Chinese Academy of Sciences, Xining, Qinghai 810001, China

ARTICLE INFO

Article history:

Accepted 29 April 2013

Available online 9 May 2013

Keywords:

Saccharopine dehydrogenase

L-Lysine biosynthesis

Density functional theory (DFT) method

Proton shuttle

Reaction mechanism

ABSTRACT

Saccharopine dehydrogenase (SDH) is the last enzyme in the AAA pathway of L-lysine biosynthesis. On the basis of crystal structures of SDH, the whole catalytic cycle of SDH has been studied by using density functional theory (DFT) method. Calculation results indicate that hydride transfer is the rate-limiting step with an energy barrier of 25.02 kcal/mol, and the overall catalytic reaction is calculated to be endothermic by 9.63 kcal/mol. Residue Lys77 is proved to be functional only in the process of saccharopine deprotonation until the formation of product L-lysine, and residue His96 is confirmed to take part in multiple proton transfer processes and can be described as a proton transfer station. From the point of view of energy, the SDH catalytic reaction for the synthesis of L-lysine is unfavorable compared with its reverse reaction for the synthesis of saccharopine. These results are essentially consistent with the experimental observations from pH dependence of kinetic parameters and isotope effects.

© 2013 Elsevier Inc. All rights reserved.

1. Introduction

As an essential amino acid for humans and animals, L-lysine can only be obtained from protein in the diet. L-Lysine can be synthesized de novo in some plants, bacteria and lower eukaryotes. Unlike other proteinogenic amino acids that have only one biosynthetic pathway, L-lysine has two distinct biosynthetic pathways, i.e., the diaminopimelate (DAP) pathway found in a wide range of plants, bacteria and lower fungi [1,2], and α -amino adipate (AAA) pathway unique to euglenoids and higher fungi [3–5]. The AAA pathway consists of eight biochemical reactions and seven enzymes, and has been found in several yeasts such as *Saccharomyces cerevisiae* [6,7], *Candida maltosa* [8] and *Penicillium chrysogenum* [9], as well as human pathogenic fungi [10,11] and plant pathogens [1,11]. As enzymes involved in AAA pathway are unique to L-lysine biosynthesis in fungal organisms [1,6,12], the selective inhibition of their activities by appropriate inhibitor can control the growth of fungal

pathogens [10,13], and they have been proved as suitable targets for rapid detection of pathogenic yeasts and molds, and for the development of antifungal drug [14].

Saccharopine dehydrogenase [N6-(glutaryl-2)-L-lysine:NAD oxidoreductase, EC 1.5.1.7] (SDH) is the last enzyme in the AAA pathway [4]. It catalyzes the reversible conversion of saccharopine to L-lysine and α -ketoglutarate (α -Kg) using NAD as an oxidant, as shown in Scheme 1 [4,15]. In the past years, the crystal structures of SDH from *S. cerevisiae* have been determined successively [16,17]. For example, the X-ray structure of wild-type SDH apoenzyme was firstly determined to a resolution of 1.6 Å in 2007 [16]. It indicates that the enzyme is composed of two similar domains with a narrow cleft between them. The active site is located at the bottom of the cleft. From the structure of active site, the authors suggest that a hingelike conformational change should be occurred firstly before the catalytic reaction because the distance between C4 of nicotinamide and C4 of saccharopine is 4.7 Å, which is too long for hydride transfer. Then, West et al. reported three ligand-bound structures in the presence of sulfate anion, adenosine monophosphate (AMP) and oxalylglycine (OxGly), respectively [17]. In the sulfate-bound structure, a sulfate ion binds in the cleft between the two domains of SDH and the cleft shows partial closure. In the AMP- and OxGly-bound structures, the ligands interact with specific residues in the active site, which represents the manner of substrate binding. Based on these structures, a semiempirical model of the SDH:NAD:saccharopine for elucidating the catalytic mechanism was proposed.

Abbreviations: DAP, diaminopimelate; AAA, α -amino adipate; SDH, saccharopine dehydrogenase; α -Kg, α -ketoglutarate; NAD, nicotinamide adenine dinucleotide [the + charge is omitted for convenience]; NADH, reduced nicotinamide adenine dinucleotide; AMP, adenosine monophosphate; OxGly, oxalylglycine.

* Corresponding author at: Key Laboratory of Theoretical and Computational Chemistry in Universities of Shandong, School of Chemistry and Chemical Engineering, Shandong University, Jinan, Shandong 250100, China. Tel.: +86 531 883 655 76; fax: +86 531 885 644 64.

E-mail address: yongjunliu.1@sdu.edu.cn (Y. Liu).

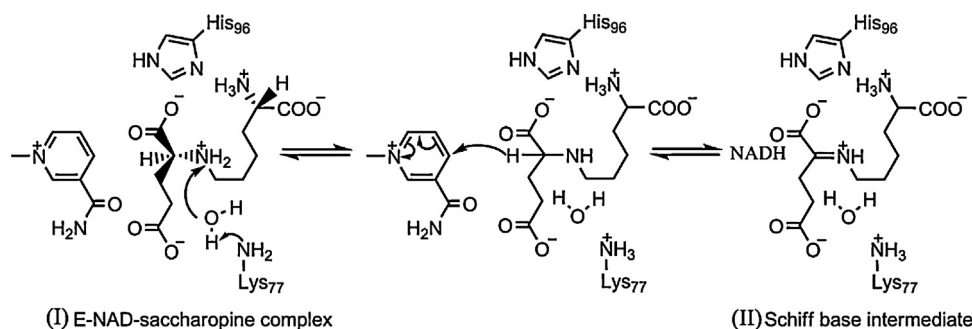


Fig. 2. The proposed pathway for the formation of Schiff base intermediate from E-NAD-saccharopine complex via water-assisted proton transfer and hydride transfer.

2. Computational details

The models used in this work were based on the recently obtained crystal structure of saccharopine dehydrogenase with closed cleft (pdb code: 3UH1) [22]. The full system includes more than 6000 atoms after added hydrogen atoms. To improve computational efficiency, our model only contains the substrate saccharopine, coenzyme NAD, a crystal water molecule and some key residues (Lys77, His96, Ala139, Ile318, Asp319, and His320). The substrate saccharopine, coenzyme and all residues are truncated, so that only important side chains or peptide backbones are included. During the optimizations, the truncated atoms were fixed to their crystallographic positions to avoid unrealistic movements of the groups involved in the model, and the fixed atoms were marked with asterisks in the corresponding figures.

There are a number of ionizable residues in the active site of SDH-NAD-saccharopine ternary complex, including Lys13, Arg18, Arg131, Lys99, Lys77, Glu122, Glu78, Glu16 and His96 [22,39–41]. The crystal structure shows that Lys77 and His96 are within hydrogen bonding distance of the secondary amine of saccharopine and could serve as acid–base catalysts in the dehydrogenase reaction. Besides, Fujioka et al. revealed SDH is a basic protein with the isoelectric pH of 10.1 [42]. SDH has pH optima of 10.0 in the direction of lysine formation and 7.0 in the direction of saccharopine formation [43]. Considering the pK_a values of Lys77, His96 and substrate (6.2, 7.2 and 10) [21] and our aim to explore the reaction mechanism of saccharopine dehydrogenase, the general acid–base Lys77 and His96 were set to their unprotonated states and substrate ϵ -amine in its protonated state.

All calculations presented here were carried out by means of the Gaussian 09 [44] program package, using hybrid density functional theory method. Geometrical structures were optimized at B3LYP/6-31G(d,p) level of theory. To obtain more accurate energies, single point calculations on the optimized structures were performed with the larger basis set 6-311++G(2d,2p), which includes diffuse functions and double polarization functions on each atom. To consider the effects of the rest of enzyme that were not included in our models on the energetics, we also used the polarizable-continuum model (PCM) [45,46] using self consistent reaction field (SCRF) model with the default UAKS radii (united atom Kohn–Sham topological model) to calculate the single point energies for each species on the optimized geometries at 6-311++G(2d,2p) level. In this model, the solvent is represented by a constant dielectric medium surrounding a cavity containing the solute. The empirical dielectric constant of the enzyme environment is chosen to be 4, which has been used in many studies [47–49]. Frequency calculations were performed with the 6-31G(d,p) basis set to obtain zero-point vibrational energies (ZPE) and to verify that all the optimized geometries correspond to a local minimum that has no imaginary frequency or a saddle point that has only one imaginary frequency. All the energies involved in this paper have included ZPE

corrections and the relative energies were reported in ΔH . Since some atoms were forced in their crystallographic positions during the structure optimization, a few small negative eigenvalues usually appear, typically in the order of 10 cm^{-1} . These frequencies do not contribute significantly to the zero-point energies and thus can be tolerated. In addition, freeze of some atoms reduces the freedom of molecule, resulting in the model slightly more rigid, and this can affect the energetics more or less. However, it was demonstrated that no alterations on the conclusions have been observed concerning the investigation of catalytic mechanism caused by these effects. All the transition states have been confirmed by intrinsic reaction coordinate (IRC) calculations [50,51].

3. Results and discussions

3.1. Formation of Schiff base intermediate (II)

As shown in Fig. 1, the overall catalytic mechanism of SDH can be divided into several parts. The catalytic cycle starts from a ternary complex (I) formed by NAD, substrate and enzyme. Previous studies on the kinetic mechanism show that NAD binds to apoenzyme firstly followed by saccharopine [52,53]. Once NAD and saccharopine bind to the enzyme, the general acid–base 1 (Lys77) accepts a proton from ϵ -amine of saccharopine. It should be noted that the water to attack the Schiff base carbon atom in the following step is located at the center of Lys77, His96 and ϵ -amine of saccharopine. It may assist the hydrogen transfer as shown in Fig. 2.

Our calculations reveal that the protonated amino denotes its proton to Lys77 firstly by the aid of water. Then the hydride of the substrate transfers to NAD to form the Schiff base intermediate (II), as shown in Fig. 2. We had tried to recognize the concerted mechanism for the formation of intermediate (II). But all attempts were failed.

The optimized structures and key parameters of the reactant (R), transition states (TS1 and TS2) and intermediates (IM1 and IM2) are shown in Fig. 3. In reactant R, some hydrogen bonds (not shown in Fig. 3) are formed between substrate saccharopine, surrounding residues and water molecule, which may greatly stabilize the active site. Significantly, the water forms three hydrogen bonds with Lys77 (r_a), saccharopine (r_c) and His96 with lengths of 1.76, 1.67 and 1.85 Å respectively. From R to IM1, a proton of water transfers to Lys77 and the proton on ϵ -amine of saccharopine transfers to water molecule in a concerted manner. In IM1, r_a and r_c are shortened to 1.07 and 1.00 Å via 1.38 and 1.11 Å in TS1, respectively, indicating the completion of the proton transfer. In TS2, the pyridine ring distorts clearly, and the distance (r_f) between the carbon atom of NAD and the hydrogen atom to be transferred changes from 2.96 to 1.34 Å. In IM2, NAD is reduced to NADH and the heterocycle returns to its original position as in IM1.

The energy profile of the whole catalytic cycle is shown in Fig. 4. One can see that the energy barrier for the formation of IM1 is

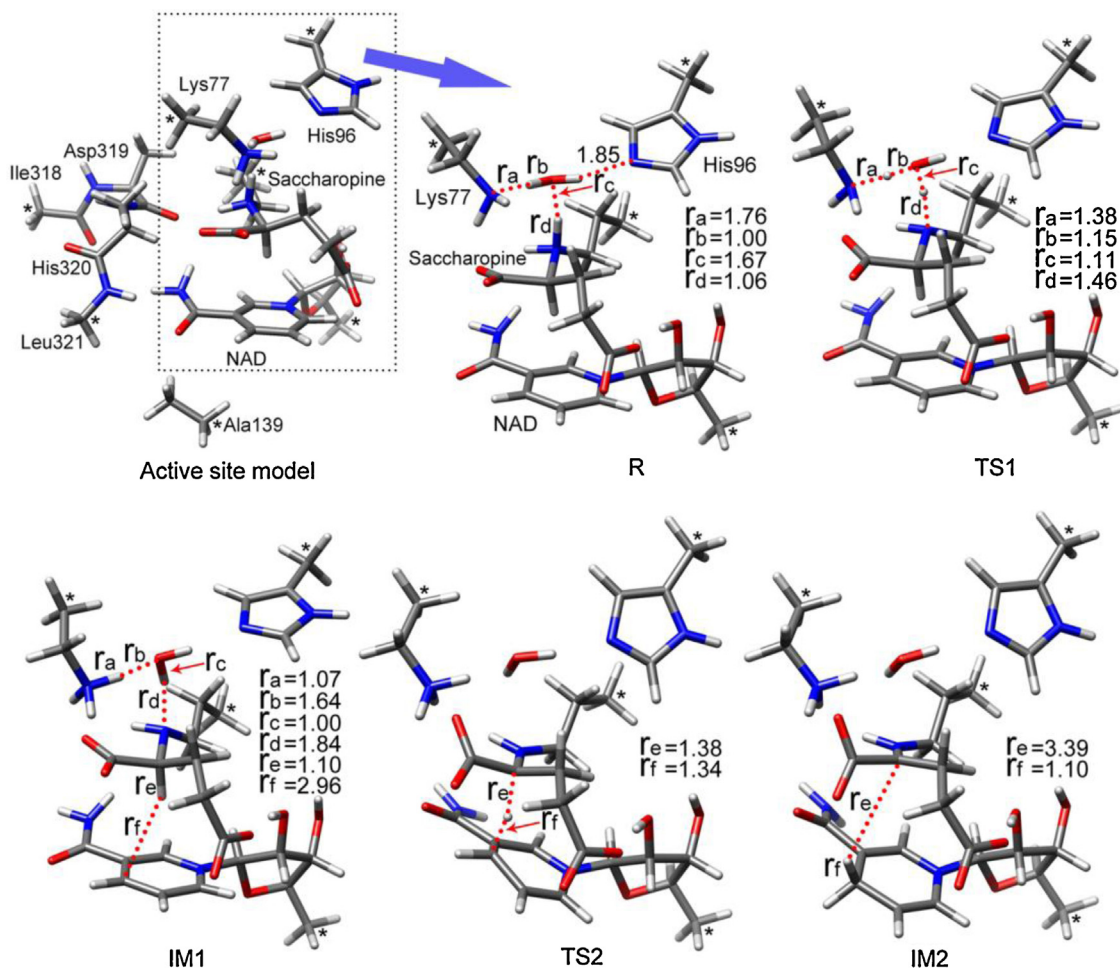


Fig. 3. Optimized geometries for various species in the formation of Schiff base intermediate via water-assisted proton transfer and hydride transfer obtained at the B3LYP/6-31G(d,p) level. Only the part in dashed box is shown in R, TS1, IM1, TS2 and IM2. The key bond distances are shown in angstrom and the fixed atoms are labeled by asterisks.

calculated to be 8.24 kcal/mol including solvation effects ($\epsilon=4$). The low barrier indicates that this proton transfer is facile. This process is slightly endothermic by 0.47 kcal/mol, implying that this intermediate IM1 is relatively stable. The subsequent hydride transfer process corresponds to an energy barrier of 25.05 kcal/mol. To examine the effect of protein electrostatic surroundings on the energy barriers, single point calculations at the level of 6-311++G(2d,2p) basis set were further performed on the optimized structures in gas phase and two solvent phases ($\epsilon=10$ and 80), which is shown in the supporting information (Fig. S1). From this energy profile, one can see that the energy barriers of proton transfer and hydride transfer decrease to 7.10 and 23.85 kcal/mol in gas

phase, respectively, while they increase 9.08 and 25.91 kcal/mol in solvent phase ($\epsilon=10$) and to 10.06 and 26.94 kcal/mol in solvent phase ($\epsilon=80$). These changes of energy barrier in different surroundings indicate that the enzyme environment exhibits clear influence on the formation of Schiff base intermediate (II). The same effect was also found in other steps (Fig. S1).

From the structural information, one can see that the proton transfer may be proceed without the assistance of water molecule, which is called direct proton transfer pathway, as shown in Fig. 5a. The calculated results are displayed in Fig. 5b, in which the optimized structures of initial reactant, transition state and intermediate are denoted as R', TS1' and IM1', respectively. In this

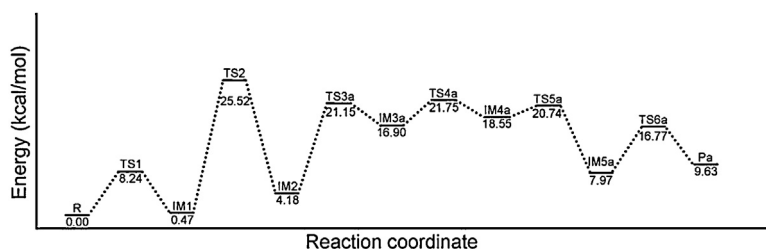


Fig. 4. Energy profile of overall reaction for the formation of L-lysine catalyzed by saccharopine dehydrogenase in solvent phase (PCM, $\epsilon=4$). The ZPE-corrected relative energies obtained at the B3LYP/6-311++G(2d,2p)//B3LYP/6-31G(d,p) level are given in kcal/mol.

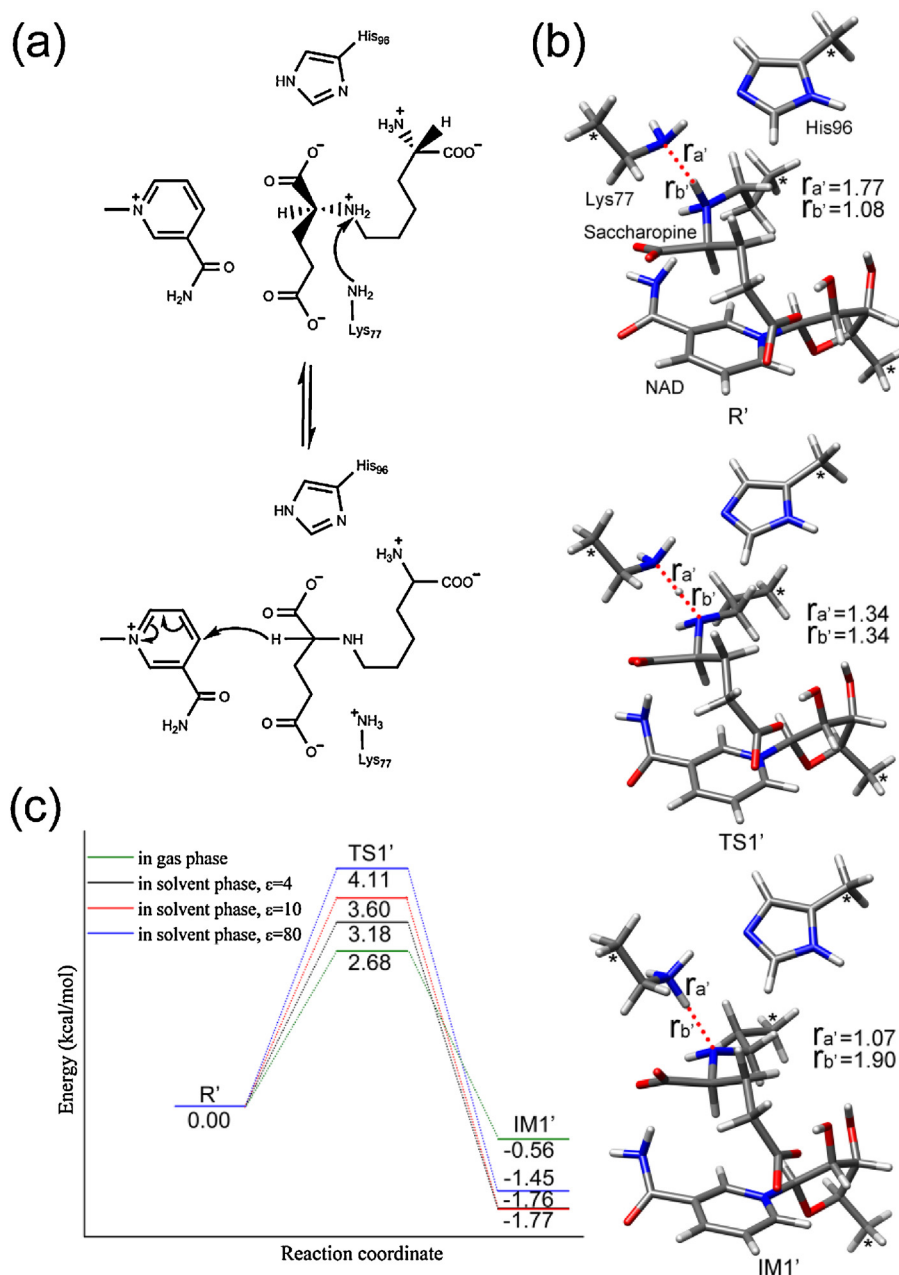


Fig. 5. Proton transfers from saccharopine to residue Lys77 via direct proton transfer pathway. (a) Catalytic mechanism; (b) optimized geometries for various species obtained at the B3LYP/6-31G(d,p) level, only the key parts of our model are shown in R', TS1', IM1'. The key bond distances are shown in angstrom and the fixed atoms are labeled by asterisks; (c) Energy profile in gas phase and solvent phase (PCM, $\epsilon = 4, 10$ and 80). The ZPE-corrected relative energies obtained at the B3LYP/6-311++G(2d,2p)//B3LYP/6-31G(d,p) level are given in kcal/mol.

pathway, the proton of ϵ -amine transfers to Lys77 without the assistance of water. In reactant R', hydrogen bonds can be also found between the substrate and residues. Among these hydrogen bonds, the one formed by Lys77 and ϵ -amine of saccharopine with a distance of 1.77 Å ($r_{a'}$) is crucial, which facilitates the proton transfer from ϵ -amine to residue Lys77. From R' to IM1', $r_{a'}$ is shortened to 1.07 Å via 1.34 Å in TS1'. The proton transfer is finished completely and the hydride transfer will occur in the next step. In addition, Lys77 always interacts with His96 by a hydrogen bond, which can be considered to stabilize the transition state and intermediate significantly.

The energy profile of the direct proton transfer pathway is given in Fig. 5c, one can see that the calculated energy barrier in solvent

phase ($\epsilon = 4$) is 3.18 kcal/mol, which decreases to 2.68 kcal/mol in gas phase and increases to 3.60 and 4.11 kcal/mol in two solvent phase ($\epsilon = 10$ and 80 , respectively). Compared with water-assisted proton transfer pathway, the energy barrier decreases by a value of about 5.0 kcal/mol. Thus, we can conclude that the water assistance cannot decrease the energy barrier of proton transfer. This can be understood by comparing the acid dissociation constants of H_2O and NH_4^+ . The acid dissociation constant at logarithmic scale pK_a values of NH_4^+ and H_2O are 9.24 and 15.7 (at 298 K) [54,55], respectively, meaning that the deprotonation of NH_4^+ is easier than that of H_2O . In the water-assisted proton transfer pathway, the concerted proton transfer involves the deprotonation process of H_2O , and thus increases the energy barrier. But the energy barriers of

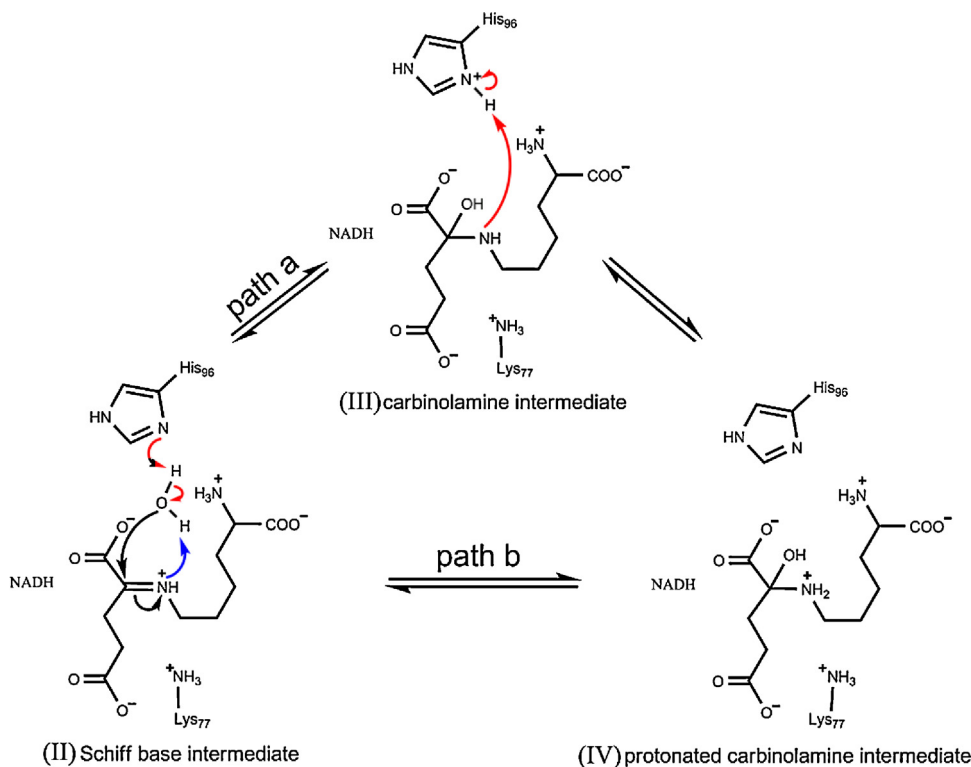


Fig. 6. Two proposed pathways for the elimination of water to give the protonated carbinolamine. Path **a** and **b** denote His96-assisted water elimination and direct water elimination, respectively. The arrows (red for path-a only and blue for path-b only) represent the direction of electron transfer. (For interpretation of the references to color in figure legend, the reader is referred to the web version of the article.)

proton transfer in both direct pathway and water-assisted pathway are all smaller than 10 kcal/mol, implying the proton transfer is easy to occur.

3.2. Formation of intermediates carbinolamine (III) and protonated carbinolamine (IV)

After the formation of Schiff base intermediate (II), the reaction undergoes the water elimination to form intermediates carbinolamine (III) and protonated carbinolamine (IV). As shown in Fig. 6, there are two possible pathways for the formation of protonated carbinolamine (IV). In path **a**, firstly, the hydroxyl of the water binds to the saccharopine and the proton transfers to His96 in a concerted manner, then the protonated His96 donates its proton to the ε-amine of saccharopine to generate the protonated carbinolamine intermediate (IV). In path **b**, the protonated carbinolamine intermediate (IV) is formed directly, i.e., His96 does not participate in the elimination of water.

The optimized structures of the species involved in pathways **a** and **b** are shown in Fig. 7. In Schiff base intermediate (IM2), the distance (r_g) between the oxygen atom of the water and the carbon atom of saccharopine is 3.71 Å. In intermediate IM3_a (the subscript **a** or **b** represents the corresponding species in paths **a** and **b**, respectively), r_g is shortened to 1.53 Å via 1.72 Å in TS3_a, suggesting the generation of C–O bond. In intermediate IM3_b, r_g is shortened to 1.39 Å via 1.56 Å in TS3_b. During the formation of C–O bond, the proton of the water transfers synchronously to the acceptor. In path **a**, the proton of water shifts to the pyrimidine ring of His96 to form the unprotonated carbinolamine, while in path **b** the proton shifts directly to the ε-amine of saccharopine leading to the formation of protonated carbinolamine. The intermediate IM3_a in path **a** then donates the proton of His96 to the ε-amine of saccharopine to generate protonated carbinolamine intermediate IM4_a via transition state TS4_a.

It should be noted that there is a minor difference on the structures of intermediates IM4_a and IM3_b due to the different orientation of newly formed OH group. In IM3_b, the OH group forms a hydrogen bond with the nitrogen atom of His96. While in IM4_a, the newly formed OH group should undergo a rotation to form the same hydrogen bond. Our calculations reveal that intermediates IM4_a could transfer to IM5_a via a transition state (TS5_a) with an energy barrier of about 2 kcal/mol (Fig. 4). In fact, IM3_b and IM5_a correspond to the identical geometrical structure.

In path **b**, the calculated energy barrier of water elimination is 48.04 (ε = 4) upon inclusion of solvation effects, which is unfavorable as catalytic reaction of enzyme. Therefore, we only discuss path **a** in the following section. The energy profile of path **a** is shown in Fig. 4. One can see that the calculated energy barrier of water elimination for the formation of carbinolamine intermediate IM3_a is lower than that of IM2 (16.97 vs 25.05 kcal/mol). Moreover, the relative energy of IM3_a is 12.72 kcal/mol higher than that of IM2. But it could easily transfer to IM5_a via two transition states, as shown in Fig. 4. IM5_a is a relatively stable intermediate in the reaction cycle.

3.3. Collapses of protonated carbinolamine (IV) to generate α-Kg and L-lysine

The collapses of protonated carbinolamine (IV) to generate α-Kg and L-lysine is the last step of catalytic cycle. As shown in Fig. 2, this step includes a C–N bond cleavage and a proton transfer. From the optimized structures shown in Fig. 7, one can see that, in TS6_a the distance (r_m) of C–N bond changes from 1.56 to 2.18 Å, while the distance (r_l) between the hydrogen atom of hydroxyl group and the nitrogen atom of His96 changes from 1.96 to 1.09 Å, indicating that the proton transfer is almost finished while the C–N bond is on the way to be broken. Downhill from the transition state TS6_a to the product P_a, r_m and r_l change to 3.88 and 1.04 Å, respectively, meaning the C–N bond has broken and the proton transfer has been

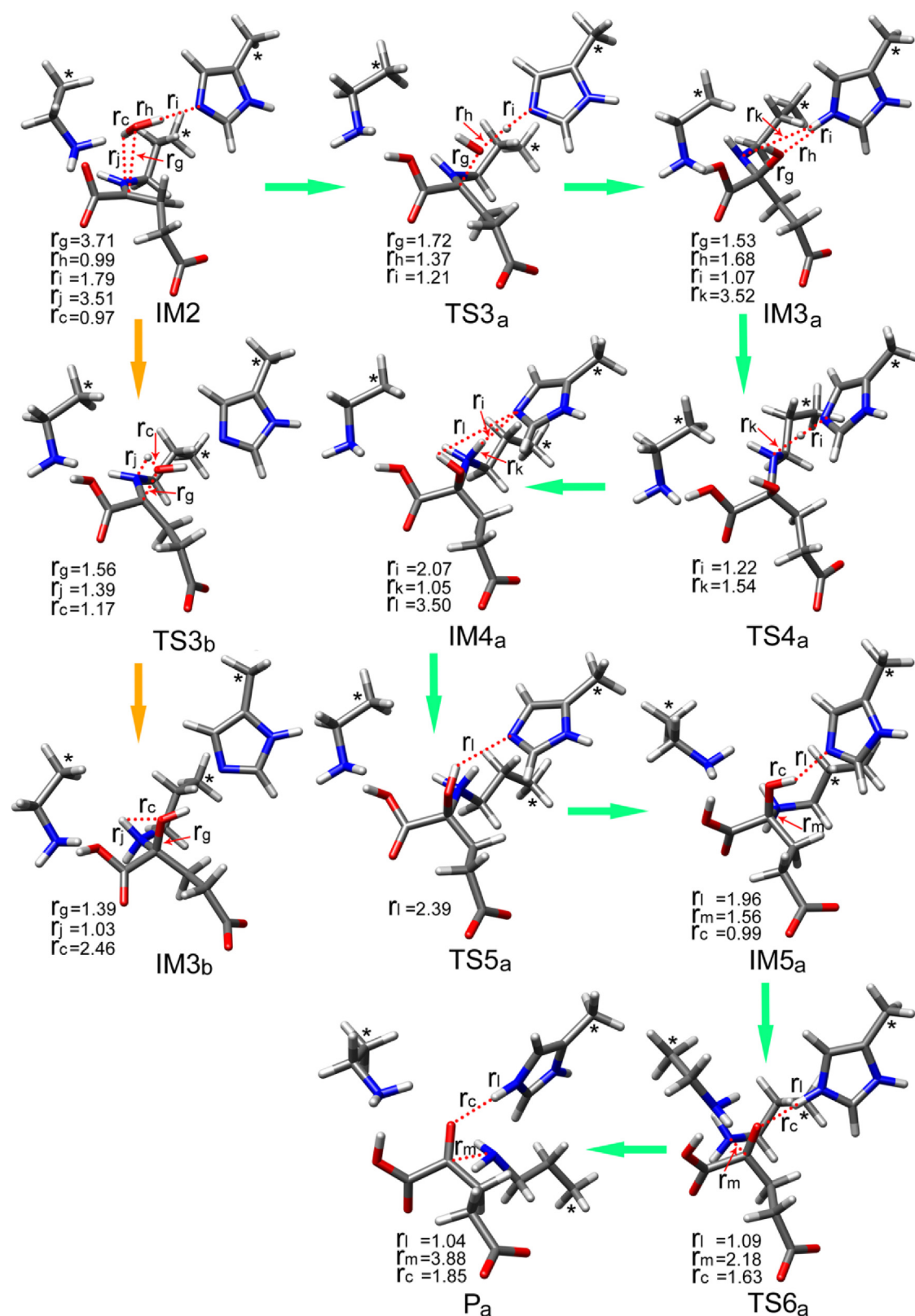


Fig. 7. Optimized geometries for various species in the two pathways of water elimination and the collapses of protonated carbinolamine obtained at the B3LYP/6-31G(d,p) level. The key bond distances are shown in angstrom and the fixed atoms are labeled by asterisks.

completely finished. Therefore, it can be concluded that this elementary reaction occurs in a concerted asynchronous mechanism and the proton transfer is prior to the cleavage of C–N bond.

From the energy profile of this step displayed in Fig. 4, one can see that the energy barrier of this concerted process is calculated to be 8.80 kcal/mol in solvent phase with $\epsilon = 4$. This process calculated to be endothermic by 1.66 kcal/mol.

4. Discussions

Above mechanistic description gives more details about the catalytic reaction and provides strong supports for the proposed mechanism. In West and Cook's works, by using multiple isotope effects and proton inventory studies [21,22], the authors suggested that the hydride transfer was major but not the sole rate-limiting step, and proton transfer steps, existing in at least two sequential transition states, also contributes to the rate-limitation. They conjectured that protons in the flight in the hydride transfer and imine hydrolysis steps completely contribute to rate limitation. According to our calculation results shown in Fig. 4, the hydride transfer from saccharopine to NAD turns out to be the most energy demanding and is the rate-limiting step. The calculated energy barrier for this process is 25.02 kcal/mol. But the water elimination only corresponds to an energy barrier of 16.67 kcal/mol. Thus, we can conclude that hydride transfer contributes to rate limitation.

It has been reported that the optimal pH value of *S. cerevisiae* enzyme is 10.0 in the direction of L-lysine formation and 7.0 in the direction of saccharopine formation [36,38]. From the energy profile shown in Fig. 4, it can be found that the reaction in the direction of L-lysine formation is endothermic by 9.63 kcal/mol. Furthermore, the calculated energy barrier of the reverse reaction of the rate-limiting hydride transfer is 21.34 kcal/mol. Therefore, the reverse reaction is more favored from energy point of view, which is in accord with the experimental results.

Furthermore, the roles of the key residues in the active site can be also illustrated by our studies. As mentioned above, Lys77, His96, Ala139, Ile318, Asp319 and His320 are all included in our models. Agreeing with the experimental results [22], residues Lys77 and His96 act as the acid–base catalysts. Residue Lys77 abstracts a proton from the saccharopine in the first step and then does not function until product L-lysine is formed at the completion of the reaction. Residue His96 firstly accepts a proton from the eliminated water and then donates it to the ϵ -amine of saccharopine. Protons shuttle between residue His96 and some other groups in three steps. Thus, residue His96 can be described as a proton transfer station. The remaining residues mainly play a role in stabilizing the transition states and intermediates.

5. Conclusions

In this paper, catalytic mechanism of saccharopine dehydrogenase has been investigated by using density functional theory (DFT) method. Details of each elementary step and the energetics of the whole catalytic cycle were determined. The calculation results indicate that proton transfer is almost involved in all steps, which is consistent with the proton shuttle mechanism proposed on the basis of experimental data. Residues Lys77 and His96 act as the acid–base catalysts. Residue Lys77 abstracts a proton in the process of saccharopine deprotonation and then does not function until product L-lysine is formed at the completion of the reaction. Residue His96 takes part in several proton transfer processes and can be described as a proton transfer station. Based on our models, the hydride transfer step is proved to be the rate-limiting step with energy barrier of 25.02 kcal/mol, and the overall catalytic reaction is endothermic by 9.63 kcal/mol. The reaction is

reverse-favored. In addition, by comparing the energy barriers of each step in gas phase and in three solvent ($\epsilon = 4, 10$ and 80) by using polarizable-continuum model (PCM), we found that the surrounding environment is crucial for this enzymatic reaction. Our results are meaningful for the design of novel inhibitors with high efficiency, and for redesign of enzyme activities for biocatalytic applications.

Acknowledgment

This work was supported by the National Natural Science Foundation of China (21173129).

Appendix A. Supplementary data

Supplementary data associated with this article can be found, in the online version, at <http://dx.doi.org/10.1016/j.jmngm.2013.04.009>.

References

- [1] H.E. Umbarger, Amino acid biosynthesis and its regulation, *Annual Review of Biochemistry* 47 (1978) 533–606.
- [2] H.J. Vogel, Two modes lysine synthesis among lower fungi: evolutionary significance, *Biochimica et Biophysica Acta* 41 (1960) 172–174.
- [3] T. Kosuge, T. Hoshino, The α -aminoacidopate pathway for lysine biosynthesis is widely distributed among *Thermus* strains, *Journal of Bioscience and Bioengineering* 88 (1999) 672–675.
- [4] H. Xu, B. Andi, J. Qian, A.H. West, P.F. Cook, The α -aminoacidopate pathway for lysine biosynthesis in fungi, *Cell Biochemistry and Biophysics* 46 (2006) 43–64.
- [5] M. Strassman, S. Weinhouse, Biosynthetic pathways. III. The biosynthesis of lysine *Torulopsis utilis*, *Journal of the American Chemical Society* 75 (1953) 1680–1684.
- [6] J.K. Bhattacharjee, Evolution of α -aminoacidopate pathway for the synthesis of lysine in fungi, in: R.P. Mortlock (Ed.), *Handbook of Evolution of Metabolic Function*, CRC Press, Boca Raton, 1992, pp. 47–80.
- [7] J.K. Bhattacharjee, M. Strassman, Accumulation of tricarboxylic acids related to lysine biosynthesis in a yeast mutant, *Journal of Biological Chemistry* 242 (1967) 2542–2546.
- [8] G. Kunze, R. Bode, H. Schmidt, I.A. Samsonova, D. Birnbaum, Identification of a *lys2* mutant of *Candida maltosa* by means of transformation, *Current Genetics* 11 (1987) 385–391.
- [9] W.M. Jaklitsch, C.P. Kubicek, Homocitrate synthase from *Penicillium chrysogenum*. Localization, purification of the cytosolic isoenzyme, and sensitivity to lysine, *Biochemical Journal* 269 (1990) 247–253.
- [10] R.C. Garrad, J.K. Bhattacharjee, Lysine biosynthesis in selected pathogenic fungi: characterization of lysine auxotrophs and the cloned *LYS1* gene of *Candida albicans*, *Journal of Bacteriology* 174 (1992) 7379–7384.
- [11] B. Andi, A.H. West, P.F. Cook, Stabilization and characterization of histidine-tagged homocitrate synthase from *Saccharomyces cerevisiae*, *Archives of Biochemistry and Biophysics* 421 (2004) 243–254.
- [12] R. Cunin, N. Glansdorff, A. Piérard, V. Stalon, Biosynthesis and metabolism of arginine in bacteria, *Microbiology Reviews* 50 (1986) 314–352.
- [13] Z.H. Ye, J.K. Bhattacharjee, Lysine biosynthesis pathway and biochemical blocks of lysine auxotrophs of *Schizosaccharomyces pombe*, *Journal of Bacteriology* 170 (1988) 5968–5970.
- [14] D.R.J. Palmer, H. Balogh, G. Ma, X. Zhou, M. Marko, S.G.W. Kaminskyj, Synthesis and antifungal properties of compounds which target the α -aminoacidopate pathway, *Pharmazie* 59 (2004) 93–98.
- [15] H. Xu, A.H. West, P.F. Cook, Determinants of substrate specificity for saccharopine dehydrogenase from *Saccharomyces cerevisiae*, *Biochemistry* 46 (2007) 7625–7636.
- [16] D.L. Burk, J. Hwang, E. Kwok, L. Marrone, V. Goodfellow, G.I. Dmitrienko, A.M. Berghuis, Structural studies of the final enzyme in the α -aminoacidopate pathway-saccharopine dehydrogenase from *Saccharomyces cerevisiae*, *Journal of Molecular Biology* 373 (2007) 745–754.
- [17] B. Andi, H. Xu, P.F. Cook, A.H. West, Crystal structures of ligand-bound saccharopine dehydrogenase from *Saccharomyces cerevisiae*, *Biochemistry* 46 (2007) 12512–12521.
- [18] M. Fujioka, Chemical mechanism of saccharopine dehydrogenase (NAD, L-lysine-forming) as deduced from initial rate pH studies, *Archives of Biochemistry and Biophysics* 230 (1984) 553–559.
- [19] M. Fujioka, Y. Takata, H. Ogawa, M. Okamoto, The inactivation of saccharopine dehydrogenase (L-lysine-forming) by diethyl pyrocarbonate, *Journal of Biological Chemistry* 255 (1979) 937–942.
- [20] H. Xu, A.H. West, P.F. Cook, Overall kinetic mechanism of saccharopine dehydrogenase from *Saccharomyces cerevisiae*, *Biochemistry* 45 (2006) 12156–12166.

- [21] H. Xu, S.S. Alguindigue, A.H. West, P.F. Cook, A proposed proton shuttle mechanism for saccharopine dehydrogenase from *Saccharomyces cerevisiae*, *Biochemistry* 46 (2007) 871–882.
- [22] V.P. Kumar, L.M. Thomas, K.D. Bobyk, B. Andi, P.F. Cook, A.H. West, Evidence in support of Lysine 77 and Histidine 96 as acid–base catalytic residues in saccharopine dehydrogenase from *Saccharomyces cerevisiae*, *Biochemistry* 51 (2012) 857–866.
- [23] J.N. Almási, E.A.C. Bushnell, J.W. Gauld, A QM/MM-based computational investigation on the catalytic mechanism of saccharopine reductase, *Molecules* 16 (2011) 8569–8589.
- [24] A.D. Becke, Density-functional exchange-energy approximation with correct asymptotic behavior, *Physical Review A* 38 (1988) 3098–3100.
- [25] A.D. Becke, Density-functional thermochemistry. I. The effect of the exchange-only gradient correction, *Journal of Chemical Physics* 96 (1992) 2155–2160.
- [26] A.D. Becke, Density-functional thermochemistry. II. The effect of the Perdew–Wang generalized-gradient correlation correction, *Journal of Chemical Physics* 97 (1992) 9173–9177.
- [27] A.D. Becke, Densityfunctional thermochemistry. III. The role of exact exchange, *Journal of Chemical Physics* 98 (1993) 5648–5652.
- [28] C. Lee, W. Yang, R.G. Parr, Development of the Colle–Salvetti correlation-energy formula into a functional of the electron density, *Physical Review B* 37 (1998) 785–789.
- [29] B. Miehlich, A. Savin, H. Stoll, H. Preuss, Results obtained with the correlation energy density functionals of Becke and Lee, Yang and Parr, *Chemical Physics Letters* 157 (1989) 200–206.
- [30] O. Méndez-Lucio, A. Romo-Mancillasa, J.L. Medina-Francob, R. Castillo, Computational study on the inhibition mechanism of cruzain by nitrile-containing molecules, *Journal of Molecular Graphics and Modelling* 35 (2012) 28–35.
- [31] M.A. Khan, R. Lo, T. Bandyopadhyay, B. Ganguly, Probing the reactivation process of sarin-inhibited acetylcholinesterase with α -nucleophiles: Hydroxylamine anion is predicted to be a better antidote with DFT calculations, *Journal of Molecular Graphics and Modelling* 29 (2011) 1039–1046.
- [32] C. Acosta-Silva, J. Bertran, V. Branchadell, A. Oliva, Quantum-mechanical study on the mechanism of peptide bond formation in the ribosome, *Journal of the American Chemical Society* 134 (2012) 5817–5831.
- [33] R.Z. Liao, J.G. Yu, F. Himo, Quantum chemical modeling of enzymatic reactions: the case of decarboxylation, *Journal of Chemical Theory and Computation* 7 (2011) 1494–1501.
- [34] M.Z. Ertem, C.J. Cramer, F. Himo, P.E.M. Siegbahn, N–O bond cleavage mechanism(s) in nitrous oxide reductase, *Journal of Biological Inorganic Chemistry* 17 (2012) 687–698.
- [35] S.F. Sousa, P.A. Fernandes, M.J. Ramos, Computational enzymatic catalysis – clarifying enzymatic mechanisms with the help of computers, *Physical Chemistry Chemical Physics* 14 (2012) 12431–12441.
- [36] D.F.A.R. Dourado, P.A. Fernandes, M.J. Ramos, Glutathione transferase classes α , π , and μ : GSH activation mechanism, *Journal of Physical Chemistry B* 114 (2010) 12972–12980.
- [37] O. Amata, T. Marino, N. Russo, M. Toscano, Human insulin-degrading enzyme working mechanism, *Journal of the American Chemical Society* 131 (2009) 14804–14811.
- [38] T. Marino, N. Russo, M. Toscano, Catalytic mechanism of the arylsulfatase promiscuous enzyme from *Pseudomonas aeruginosa*, *Chemistry–A European Journal* 19 (2013) 2185–2192.
- [39] D.K. Ekanayake, A.H. West, P.F. Cook, Contribution of K99 and D319 to substrate binding and catalysis in the saccharopine dehydrogenase reaction, *Archives of Biochemistry and Biophysics* 514 (2011) 8–15.
- [40] D.K. Ekanayake, B. Andi, K.D. Bobyk, A.H. West, P.F. Cook, Glutamates 78 and 122 in the active site of saccharopine dehydrogenase contribute to reactant binding and modulate the basicity of the acid–base catalysts, *Journal of Biological Chemistry* 285 (2010) 20756–20768.
- [41] V.P. Kumar, A.H. West, P.F. Cook, Supporting role of lysine 13 and glutamate 16 in the acid–base mechanism of saccharopine dehydrogenase from *Saccharomyces cerevisiae*, *Archives of Biochemistry and Biophysics* 522 (2012) 57–61.
- [42] H. Ogawa, M. Fujioka, Purification and characterization of saccharopine dehydrogenase from baker's yeast, *Journal of Biological Chemistry* 253 (1978) 1670–1666.
- [43] T.M. Zabriskie, M.D. Jackson, Lysine biosynthesis and metabolism in fungi, *Natural Product Reports* 17 (2000) 85–97.
- [44] M.J. Frisch, G.W. Trucks, H.B. Schlegel, G.E. Scuseria, M.A. Robb, J.R. Cheeseman, G. Scalmani, V. Barone, B. Mennucci, G.A. Petersson, H. Nakatsuji, M. Caricato, X. Li, H.P. Hratchian, A.F. Izmaylov, J. Bloino, G. Zheng, J.L. Sonnenberg, M. Hada, M. Ehara, K. Toyota, R. Fukuda, J. Hasegawa, M. Ishida, T. Nakajima, Y. Honda, O. Kitao, H. Nakai, T. Vreven, J.A. Montgomery Jr., J.E. Peralta, F. Ogliaro, M. Bearpark, J.J. Heyd, E. Brothers, K.N. Kudin, V.N. Staroverov, T. Keith, R. Kobayashi, J. Normand, K. Raghavachari, A. Rendell, J.C. Burant, S.S. Iyengar, J. Tomasi, M. Cossi, N. Rega, J.M. Millam, M. Klene, J.E. Knox, J.B. Cross, V. Bakken, C. Adamo, J. Jaramillo, R. Gomperts, R.E. Stratmann, O. Yazyev, A.J. Austin, R. Cammi, C. Pomelli, J.W. Ochterski, R.L. Martin, K. Morokuma, V.G. Zakrzewski, G.A. Voth, P. Salvador, J.J. Dannenberg, S. Dapprich, A.D. Daniels, O. Farkas, J.B. Foresman, J.V. Ortiz, J. Cioslowski, D.J. Fox, Gaussian 09 (Revision B.01), Gaussian Inc., Wallingford CT, 2010.
- [45] V. Barone, M. Cossi, J. Tomasi, Geometry optimization of molecular structures in solution by the polarizable continuum model, *Journal of Computational Chemistry* 19 (1998) 404–417.
- [46] J. Tomasi, M. Persico, Molecular interactions in solution: an overview of methods based on continuous distributions of the solvent, *Chemical Reviews* 94 (1994) 2027–2094.
- [47] M.R.A. Blomberg, P.E.M. Siegbahn, G.T. Babcock, Modeling electron transfer in biochemistry: a quantum chemical study of charge separation in *Rhodospirillum rubrum* Photosystem II, *Journal of the American Chemical Society* 120 (1998) 8812–8824.
- [48] J.J. Robinet, K.B. Cho, J.W. Gauld, A density functional theory investigation on the mechanism of the second half-reaction of nitric oxide synthase, *Journal of the American Chemical Society* 130 (2008) 3328–3334.
- [49] R.J. Liao, W.J. Ding, J.G. Yu, W.H. Fang, R.Z. Liu, Theoretical studies on pyridoxal 5'-phosphate-dependent transamination of α -amino acids, *Journal of Computational Chemistry* 29 (2008) 1919–1929.
- [50] C. Gonzalez, H.B. Schlegel, An improved algorithm for reaction path following, *Journal of Chemical Physics* 90 (1989) 2154–2161.
- [51] C. Gonzalez, H.B. Schlegel, Reaction path following in mass-weighted internal coordinates, *Journal of Physical Chemistry* 94 (1990) 5523–5527.
- [52] M. Fujioka, Y. Nakatani, A kinetic study of saccharopine dehydrogenase reaction, *European Journal of Biochemistry* 16 (1970) 180–186.
- [53] M. Fujioka, Y. Nakatani, Saccharopine dehydrogenase: interaction with substrate analogues, *European Journal of Biochemistry* 25 (1972) 301–307.
- [54] A. Albert, E.P. Serjeant, Ionization Constants of Acids and Bases: A Laboratory Manual, Methuen, London, 1962.
- [55] W.P. Jencks, J. Regenstein, Ionization constants of acids and bases, in: G.D. Fasman (Ed.), *Handbook of Biochemistry and Molecular Biology*, CRC Press, Boca Raton, 1976, pp. 305–351.